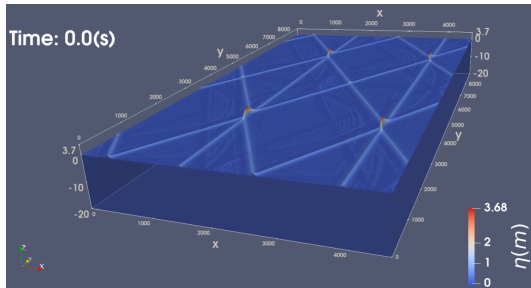


Nonlinear water-wave and wave-impact dynamics using variational principles and automated numerics in Firedrake

Onno Bokhove & Mark Kelmanson; EU-GA859983

Leeds Institute for Fluid Dynamics –[MARIN seminar 21-04-2023](#)



1. Motivation on modelling extremely high water waves

- Origin 2010 *bore-soliton-splash*:
- To what extent do exact but idealised extreme- or rogue-wave solutions survive in more realistic settings?
- Will such extreme waves fall apart due to dispersion or other mechanisms?
- Use fourfold and ninefold KP amplifications of interacting solitons/cnoidal waves.
- What do you think: will we be **able to reach the ninefold wave amplification** in more realistic calculations, using potential-flow dynamics, or in reality?

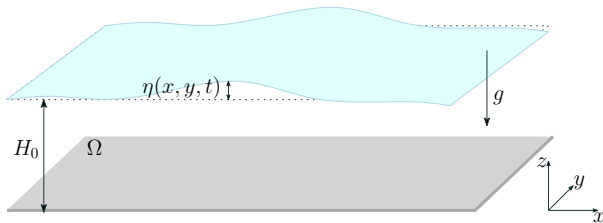


1. Motivation: statements & goals

- Nonlinear water-wave & wave-impact dynamics on wind-turbine masts succinctly **described by variational principles (VPs)**; advantageous theoretical interconnectivity with conservation laws.
- Mathematical modelling based on VPs allows inclusion of simple dissipation, **piston wavemakers and waveflaps**.
- **VPs can be directly implemented** numerically into FEM framework “**Firedrake**”, advantageous in moving domains and reduction in development time.
- *Ex. 1:* 3D nonlinear potential-flow code **extreme-wave interactions** of cnoidal/solitary waves.
- *Ex. 2:* 2D nonlinear potential-flow code with **waveflap**.
- *Ex. 3:* **FSI** generalised coordinate-transformation asymptotics for nonlinear wind-turbine motion.

2. Mathematical hierarchy: potential-flow theory

Velocity potential $\phi(x, y, z, t)$, defined by $\mathbf{u} = \nabla\phi$ (irrotational flow)



Water-wave equations (PFE)

$$\nabla^2\phi = 0 \quad \text{in } \Omega$$

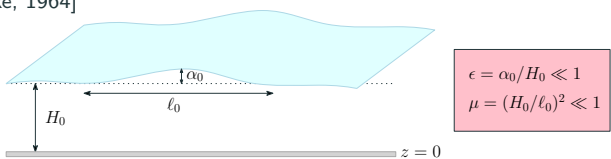
$$\partial_t\eta + \nabla\phi \cdot \nabla\eta - \partial_z\phi = 0 \quad \text{at } z = H_0 + \eta$$

$$\partial_t\phi + \frac{1}{2}|\nabla\phi|^2 + g\eta = 0 \quad \text{at } z = H_0 + \eta$$

$$\mathbf{n} \cdot \nabla\phi = 0 \quad \text{on } z = 0 \text{ and } \partial\Omega$$

2. Mathematical hierarchy: BLE and KPE approximations

- ~ Shallow water approximation: long wave length compared to mean water depth
- ~ Boussinesq approximation: includes weak dispersive effects
 - KdV equation: wave propagation in 1D [Korteweg & de Vries, 1895]
 - KP equation: unidirectional propagation in 2DH [Kadomtsev & Petviashvili, 1970]
 - Benney-Luke equations: bidirectional propagation in 2DH [Benney & Luke, 1964]



Expansion about the sea-bed potential $\Phi(x, y, t) = \phi(x, y, z = 0, t)$, in powers of the small parameter μ [Pego & Quintero, 1999]

Benney-Luke equations (BLE)

$$\begin{aligned}\partial_t \eta - \frac{\mu}{2} \partial_t \nabla^2 \eta + \nabla \cdot ((1 + \epsilon \eta) \nabla \Phi) - \frac{2\mu}{3} \nabla^4 \Phi &= 0 && \text{in } \Omega \\ \partial_t \Phi - \frac{\mu}{2} \partial_t \nabla^2 \Phi + \frac{\epsilon}{2} |\nabla \Phi|^2 + \eta &= 0 && \text{in } \Omega \\ \mathbf{n} \cdot \nabla \Phi &= 0 && \text{on } \partial\Omega \\ \mathbf{n} \cdot \nabla (\nabla^2 \Phi) &= 0 && \text{on } \partial\Omega\end{aligned}$$

Total Energy

$$E(t) = \int_{\Omega} \left(\frac{1}{2} \eta^2 + \frac{1}{2} (1 + \epsilon \eta) |\nabla \Phi|^2 + \frac{\mu}{3} (\nabla^2 \Phi)^2 \right) dx dy$$

is conserved in time due to the Hamiltonian nature of the system

[Bokhove & Kalogirou, 2016]

Kadomtsev-Petviashvili equation (KPE)

The KPE can be obtained from the BLE by introducing the formal perturbation expansions

$$\eta = \tilde{u} + \mathcal{O}(\epsilon^2), \quad \Phi = \sqrt{\epsilon} \left(\tilde{\Psi} + \mathcal{O}(\epsilon^2) \right),$$

using the transformations

$$X = \sqrt{\frac{\epsilon}{\mu}} \left(\frac{3}{\sqrt{2}} \right)^{1/3} (x - t), \quad Y = \sqrt{\epsilon} \sqrt{\frac{\epsilon}{\mu}} \left(\frac{3}{\sqrt{2}} \right)^{2/3} y,$$
$$\tau = \epsilon \sqrt{\frac{2\epsilon}{\mu}} t, \quad u = \left(\frac{3}{4} \right)^{1/3} \tilde{u},$$

and taking $\mu = \epsilon^2$, resulting in the KPE in “standard” form

$$\partial_X (4\partial_\tau u + 6u\partial_X u + \partial_{XXX} u) + 3\partial_{YY} u = 0$$

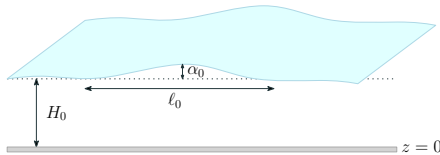
This equation includes weak dispersion effects in the y -direction.

3. Wave dynamics and variational principles (VPs)

Why VPs? Compact formulation, conservation laws, numerically advantageous.

~ Examples:

- Linear shallow-water dynamics (pedagogical example).
- **Benney-Luke equations –BLE**: bidirectional propagation in 2DH, Boussinesq-type model [Benney & Luke, 1964].
- **Potential-flow equations –PFE**: 3D [Luke 1967].



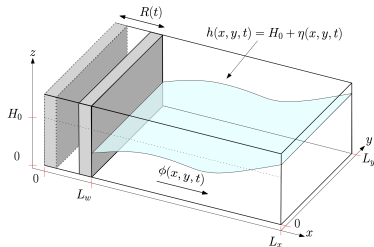
$$\epsilon = \alpha_0 / H_0 \ll 1$$
$$\mu = (H_0 / \ell_0)^2 \ll 1$$

VP linear shallow-water dynamics

- In 1D, VP for linear & shallow-water dynamics is:

$$\begin{aligned} 0 &= \delta \int_0^T \mathcal{L}_{swe}[\phi, \eta] dt \\ &= \delta \int_0^T \int_0^L \phi \partial_t \eta - \frac{1}{2} H_0 |\partial_x \phi|^2 - \frac{1}{2} g \eta^2 dx - H_0 \dot{R} \phi|_{x=0} dt \end{aligned}$$

- Piston wavemaker at $x = R(t)$ is linearised around $x = 0$.
- Firedrake: directly program time-discrete version of VP.



VP for linear shallow-water dynamics

- Variations defined by:

$$\delta \mathcal{L}_{swe}[\phi, \eta] \equiv \lim_{\epsilon \rightarrow 0} \frac{\mathcal{L}_{swe}[\phi + \epsilon \delta \phi, \eta + \epsilon \delta \eta] - \mathcal{L}_{swe}[\phi, \eta]}{\epsilon}$$

- Equations of motion (continuity & Bernoulli eqns plus BCs):

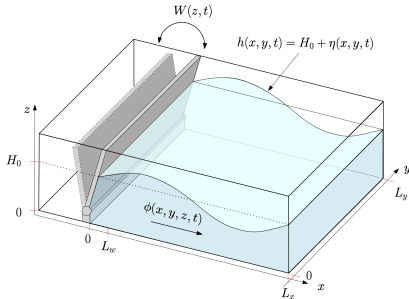
$$\begin{aligned}\partial_t h &= \partial_t \eta = -\partial_x (H_0 \partial_x \phi), \\ \partial_t \phi &= -g \eta \\ \partial_x \phi &= \dot{R} \quad \text{at} \quad x = 0, \quad \text{and} \\ \partial_x \phi &= 0 \quad \text{at} \quad x = L.\end{aligned}\tag{1}$$

VP for 2D potential-flow with waveflap

- Luke's (1967) VP –**issue** is parameterisation of domain:

$$0 = \delta \int_0^T \mathcal{L}[\phi, h] dt = \delta \int_0^T \iiint_{\Omega} \partial_t \phi + \frac{1}{2} |\nabla \phi|^2 + g(z - H_0) dz dx dy dt. \quad (2)$$

- VP quite **involved/horrendous** in transformed fixed domain.



VP for 2D potential-flow with waveflap

- VP quite involved/horrendous after transformation to coordinates in a fixed domain (equations really involved):

$$\begin{aligned} z &= \zeta h / H_0, \quad x_\xi = \frac{(L_w - W)}{L_w} + \frac{\zeta}{H_0} W_z \frac{(L_w - \xi)}{L_w} h_\xi, \\ x_\zeta &= \frac{(L_w - \xi)}{L_w} W_z \frac{h}{H_0}, z_\xi = \zeta h_\xi / H_0, \quad z_\zeta = h / H_0, \\ W &= W(\zeta h / H_0, \tau), \quad W_\tau = \partial_\tau W(z, \tau)|_{z=\zeta h / H_0}, \\ W_z &= \partial_z W(z, \tau)|_{z=\zeta h / H_0}, \quad |J| = x_\xi z_\zeta - x_\zeta z_\xi \\ 0 &= \delta \int_0^T \int_0^{L_s} \left(-(1 - W/L_w) \phi h_\tau + (1 - \xi/L_w) h_\xi W_\tau \phi \right. \\ &\quad \left. + x_\xi g \left(\frac{1}{2} z^2 - H_0 z \right) \Big|_{\zeta=H_0} \right) d\xi \\ &\quad + \int_0^{H_0} \left(z_\zeta W_\tau \phi + x_\xi g \left(\frac{1}{2} z^2 - H_0 z \right) \Big|_{\xi=0} \right) d\zeta \\ &\quad + \int_0^{L_s} \int_0^{H_0} \frac{1}{2|J|} \left((x_\zeta^2 + z_\zeta^2) |\partial_\xi \phi|^2 \right. \\ &\quad \left. - 2(x_\xi x_\zeta + z_\xi z_\zeta) \partial_\xi \phi \partial_\zeta \phi \right. \\ &\quad \left. + (x_\xi^2 + z_\xi^2) |\partial_\zeta \phi|^2 \right) d\xi d\zeta d\tau. \end{aligned}$$

VP for 3D potential-flow dynamics in x -periodic domain

- VP in 3D quite involved after coordinate transformation into fixed domain, eqn. (8) in Gidel, Lu et al. (2022).
- Partition $\mathbf{u} = \nabla\phi$ into $\phi(x, y, z, t) = \psi(x, y, t)\hat{\phi}(z) + \varphi(x, y, z, t)$ with $\hat{\phi}|_{z=H_0} = 1$, $\varphi|_{z=H_0} = 0$; VP:

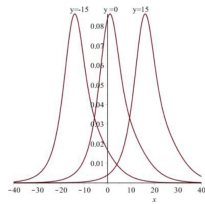
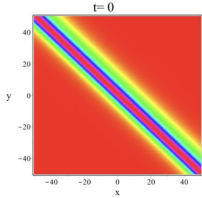
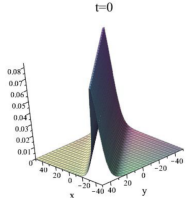
$$\begin{aligned} 0 = & \delta \int_0^T \int_{\hat{\Omega}_{x,y}} \left[\left(-H_0 \psi \partial_t h + H_0 g h \left(\frac{1}{2} h - H_0 \right) \right. \right. \\ & + \int_0^{H_0} \left[\frac{1}{2} h \left(\psi_x \hat{\phi} + \varphi_x - \frac{z h_x}{h} (\psi \hat{\phi}_z + \varphi_z) \right)^2 \right. \\ & + \frac{1}{2} h \left(\psi_y \hat{\phi} + \varphi_y - \frac{z h_y}{h} (\psi \hat{\phi}_z + \varphi_z) \right)^2 \\ & \left. \left. + \frac{1}{2} \frac{H_0^2}{h} (\psi \hat{\phi}_z + \varphi_z)^2 \right] dz \right] dx dy dt, \end{aligned} \quad (3)$$

4. Exact 1-2-3 line solitons –SP1

Single line solitons have $(N, M) = (1, 2)$, resulting in $K = f_1 = e^{\theta_1} + e^{\theta_2}$ and the line soliton solution is

$$\begin{aligned} u(X, Y, \tau) &= 2\partial_{XX} \ln K(X, Y, \tau) = \frac{1}{2}(k_1 - k_2)^2 \operatorname{sech}^2 \frac{1}{2}(\theta_1 - \theta_2) \\ &= \frac{1}{2}(k_1 - k_2)^2 \operatorname{sech}^2 \frac{1}{2}((k_1 - k_2)X + (k_1^2 - k_2^2)Y - (k_1^3 - k_2^3)\tau). \end{aligned}$$

The soliton amplitude is $\tilde{A} = \frac{1}{2}(k_1 - k_2)^2$ and its centreline is found by setting the sech^2 argument to zero.



4. Example: two interacting line solitons –SP2

Two line solitons have $(N, M) = (2, 4)$, also called $(2, 2)$ -solitons or O -solitons, obtained with functions $f_1 = e^{\theta_1} + e^{\theta_2}$, $f_2 = e^{\theta_3} + e^{\theta_4}$, and

$$K(X, Y, \tau) = (k_3 - k_1)e^{\theta_1 + \theta_3} + (k_3 - k_2)e^{\theta_2 + \theta_3} + (k_4 - k_1)e^{\theta_1 + \theta_4} + (k_4 - k_2)e^{\theta_2 + \theta_4}.$$

In the far field $Y \rightarrow \pm\infty$, we find the single line solitons

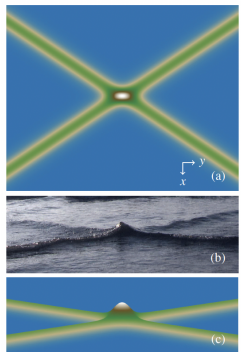
$$u_{[1,2]}(X, Y, \tau) = \frac{1}{2}(k_2 - k_1)^2 \operatorname{sech}^2 \frac{1}{2}(\theta_1 - \theta_2 - \ln a),$$

$$u_{[3,4]}(X, Y, \tau) = \frac{1}{2}(k_4 - k_3)^2 \operatorname{sech}^2 \frac{1}{2}(\theta_3 - \theta_4 - \ln b),$$

where a, b depend on k_j . For equal far-field soliton amplitudes $\tilde{A} = \frac{1}{2}(k_2 - k_1)^2 = \frac{1}{2}(k_4 - k_3)^2$, the solution satisfies [Kodama, 2010]

$$2\tilde{A} \leq \max_{(X, Y, \tau)} u(X, Y, \tau) \leq 2 \left(1 + \frac{1 - \sqrt{\Delta_o}}{1 + \sqrt{\Delta_o}} \right) \tilde{A},$$

where $0 \leq \Delta_o \leq 1$, hence $2\tilde{A} \leq \max u \leq 4\tilde{A}$.



4. Example: three interacting line solitons –SP3

Three line solitons, known as (3, 3)-solitons, have $(N, M) = (3, 6)$ and functions $f_1 = e^{\theta_1} + e^{\theta_2}$, $f_2 = e^{\theta_3} + e^{\theta_4}$, $f_3 = e^{\theta_5} + e^{\theta_6}$, and

$$K(X, Y, \tau) = \underbrace{A_{135}}_{e^{\theta_1+\theta_3+\theta_5}} e^{\theta_1+\theta_3+\theta_5} + \underbrace{A_{235}}_{e^{\theta_2+\theta_3+\theta_5}} e^{\theta_2+\theta_3+\theta_5} + \underbrace{A_{136}}_{e^{\theta_1+\theta_3+\theta_6}} e^{\theta_1+\theta_3+\theta_6} + A_{236} e^{\theta_2+\theta_3+\theta_6} \\ + A_{145} e^{\theta_1+\theta_4+\theta_5} + \underbrace{A_{245}}_{e^{\theta_2+\theta_4+\theta_5}} e^{\theta_2+\theta_4+\theta_5} + \underbrace{A_{146}}_{e^{\theta_1+\theta_4+\theta_6}} e^{\theta_1+\theta_4+\theta_6} + \underbrace{A_{246}}_{e^{\theta_2+\theta_4+\theta_6}} e^{\theta_2+\theta_4+\theta_6},$$

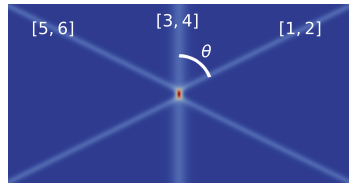
with the following parameter ordering $k_1 < k_2 < k_3 < 0 < k_4 < k_5 < k_6$.

In the far field $Y \rightarrow \pm\infty$, we find the single line solitons

$$u_{[1,2]} \approx \frac{1}{2}(k_2 - k_1)^2 \operatorname{sech}^2 \frac{1}{2}(\theta_1 - \theta_2 - \ln \tilde{a}),$$

$$u_{[5,6]} \approx \frac{1}{2}(k_6 - k_5)^2 \operatorname{sech}^2 \frac{1}{2}(\theta_5 - \theta_6 - \ln \tilde{b}),$$

$$u_{[3,4]} \approx \frac{1}{2}(k_4 - k_3)^2 \operatorname{sech}^2 \frac{1}{2}(\theta_3 - \theta_4),$$



with $\theta_i - \theta_j = (k_i - k_j) \left(X + (k_i + k_j)Y - (k_i^2 + k_i k_j + k_j^2)\tau \right)$.

Example: three interacting line solitons

Parameters k_1, \dots, k_6 are determined from

$$k_3 + k_4 = 0$$

$$k_5 + k_6 = -(k_1 + k_2) = \tan \theta$$

$$k_4 - k_3 = \sqrt{2\tilde{A}}$$

$$k_6 - k_5 = k_2 - k_1 = \sqrt{2\tilde{A}/\lambda}$$

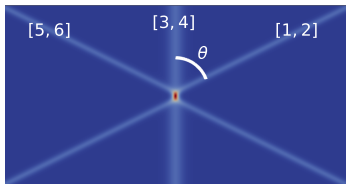
where angle $\theta > 0$,
 $\tilde{A} = \frac{1}{2}(k_4 - k_3)^2$ is the
amplitude of the [3, 4]
soliton, and the outer two
solitons are assumed to have
amplitude \tilde{A}/λ , for $\lambda \geq 1$.

Solving the above six equations, gives

$$k_6 = -k_1 = \sqrt{\tilde{A}} \left(\sqrt{2/\lambda} + \sqrt{1/2} + \delta \right)$$

$$k_5 = -k_2 = \sqrt{\tilde{A}} \left(\sqrt{1/2} + \delta \right)$$

$$k_4 = -k_3 = \sqrt{\tilde{A}/2},$$

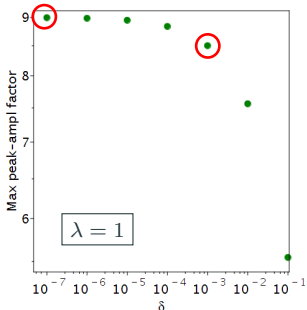
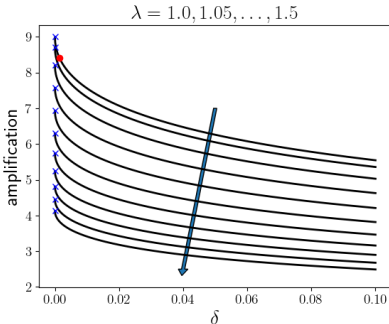


where δ is defined by

$$\delta = \frac{\tan \theta}{2\sqrt{\tilde{A}}} - \left(\sqrt{1/2\lambda} + \sqrt{1/2} \right) > 0.$$

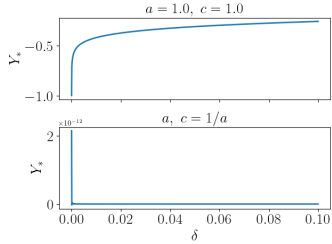
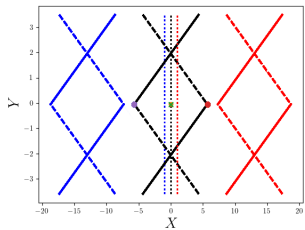
Maximum 9-fold amplification in KP

- Proof is based on a **geometric argument** (additional secondary proof)
- Find **5 centrelines** of each of three line solitons (no phase shift at peak)
- Look for intersection points \rightsquigarrow this gives two values of Y , with mean at a unique point $Y_{*\delta \rightarrow 0} \rightarrow -\infty$ when $\tau_* = 0$ and $X_* = 0$
- The space-time point of maximum amplification is (X_*, Y_*, τ_*)
- Amplification:**
$$\frac{u(X_*, Y_*, \tau_*)}{\tilde{A}} = \frac{(\sqrt{\lambda} + 2)^2}{\lambda} + \mathcal{O}(\sqrt{\delta}) \xrightarrow[\delta=0]{} 1 + \frac{4}{\lambda} + \frac{4}{\sqrt{\lambda}}$$



Proof of maximum 9-fold amplification in KP

- Three shift parameters $a, b = 1, c = 1/a$ can be optimised such that splash occurs at $(X^*, Y^*, \tau^*) = (0, 0, 0)$.
- Amplification**
 $u(X^*, Y^*, \tau^*)/\tilde{A} = 9 - 8\sqrt{3}\sqrt[4]{2}\sqrt{\delta} + 16\sqrt{2}\delta - 192^{3/4}\sqrt{3}\delta^{3/2}/3$
- Principle Minor Theorem proofs** that (X^*, Y^*, τ^*) is a maximum.
- Involved and combined geometrical and analytical proofs.



5. Firedrake: numerical implementation



Firedrake

An automated system for the solution of PDEs using the Finite Element Method (FEM).

Firedrake employs Unified Form Language (UFL) and linear & non-linear solvers PETSc solvers [Rathgeber et al., 2016].

- Space-time discretisation 2nd, 4th order of VP for BLE:
bounded energy oscillations, phase-space conserved.
- Continuous Galerkin (CG) FEM in space for VP, with
approximations & test functions/variations $\delta\eta_h$, $\delta\Phi_h$:

$$\eta(x, y, t) \approx \eta_h(x, y, t) = \sum_k \eta_k(t) w_k(x, y), \dots$$

- Symplectic Störmer-Verlet & MMP time-stepping schemes.
- **Stable numerical scheme:** no artificial amplitude damping ...

5. Firedrake: exciting aspects & VPs

- “**Firedrake**” offers continuous and discontinuous Galerkin FEM, with various types of basis functions, mesh types (gmsh, extruded meshes) focussed on applications in Geophysical and Geological Fluid Dynamics. Comparable with “**Fenics**”.
- Firedrake has (automated) MPI-HPC, various preconditioners and also time-integration options.
- Generally, the (time-discrete) **weak forms** of a system of equations are implemented.
- The **exciting novel & pursued** development is to implement (time-discrete) VPs directly, whereafter weak forms are generated automatically via command “*derivative*”.

Firedrake: exciting aspects & VPs

- The **exciting novel & pursued** development is to implement (time-discrete) VPs directly via command “*derivative*”.
- Advantages: stunning **reduction time-to-development**; 3D potential-flow code in few days, 2D potential-flow code with waveflap in a few months (by OB with help of JC).
- Compare with **years** it took for Floriane Gidel to develop (2015-2018) geometric potential-flow version of Bingham/Engsig-Karups PFE model (and Gagarina’s).
- **New codes more versatile**: horizontal mesh with spectral GLL combined with (i) vertical elements with GLL or (ii) 1 vertical element with high-order spectral GLL.

Firedrake: exciting aspects & VPs –further developments

- New codes more versatile: horizontal spectral GLL with (i) vertical GLL-elements or (ii) 1 vertical high-order spectral GLL element; strategy/comparison needed.
- HPC-MPI immediately available (Junho Choi), preconditioners (Colin Cotter): hitherto speed-up of $3.7\times$ to $8.75\times$.
- Include *h* or *p* multigrid.
- Compare approach with one with weak-forms for BLE and PFE, verifications and validations.

6. Simulation of 2D wave off waveflap –steps

Time-discrete VP using modified midpoint scheme directly typed in, as phonetic script, into Firedrake:

- time-discrete VP,
- use “derivative” command 3× with respect to 3 variables $\psi^{n+1/2}, \eta^{n+1/2}, \varphi^{n+1/2}$,
- combine into one solver call with solver-parameters,
- time loop with plotting & saving data,
- perform MPI-HPC call,
- do plotting,
- (nearly) done.
- . . . piston-wave limit (done), then full waveflap; to do: verification & validation.

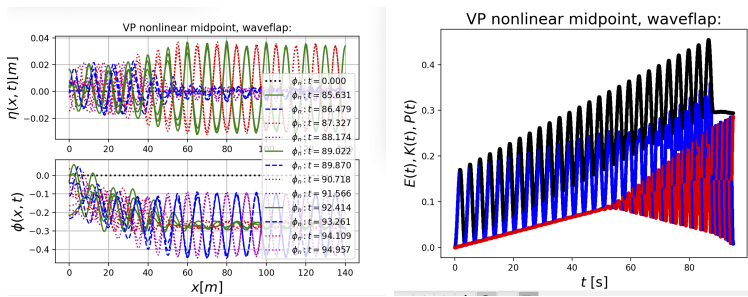
6. Simulation of 2D wave off waveflap –code

Time-discrete VP using modified midpoint scheme directly typed in; “*UFL is fully decomposable*” (CC):

```
VPnl = (-fd.inner(phimp, (eta_new - eta)/dt) + fd.inner(etamp, (phiii - phi_f)/dt)
+ Fpsi0 * (1.0 - x[0]/Lw) * (dRwavedt + FtnWM * dWflapdts) * etamp.dx(0))
* fd.dst(degree = vpoly)
+ 0.5 * (1.0/FJacobian) * ((Fdxdxi3 ** 2 + Fdzdx3 ** 2) * (Fdpsidxi0 * phihat + varphimp.dx(0)) *
(Fpsi0 * phihat.dx(1) + varphimp.dx(1))
+ (Fdxdxi ** 2 + Fdzdx3 ** 2) * (Fpsi0 * phihat.dx(1) + varphimp.dx(1)) ** 2)
* fd.dx(degree = (vpoly))
+ gg * FJacobian * (Fz - H0x) * fd.dx(degree = (vpoly))
+ (Fdxdxi3 * (dRwavedt + FtnWM * dWflapdts) * (Fpsi0 * phihat + varphimp))
* fd.ds_v(1, degree = vpoly)
...
phif_exprnl1 = fd.derivative(VPnl, phimp, du = vvmp0)
...
phi_combonl = fd.NonlinearVariationalSolver(fd.NonlinearVariationalProblem(
Fexprnl, result_mixedmp, bcs = BC_varphi_mixedmp),
solver_parameters = lines_parameters)
```

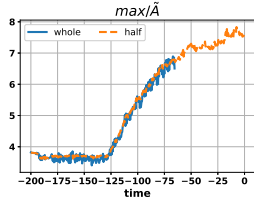
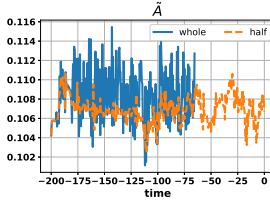
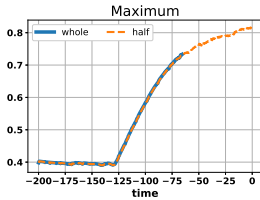
6. Simulation of 2D wave off waveflap –Preliminary results

Profiles and energy, regular (standing) waves generated by waveflap switched off after $28T_p$ (Rehman et al. OMAE2023):



7. Simulation of extreme waves

- KPE solutions hold on infinite horizontal plane, so domain has to be sufficiently large to eliminate reflection at boundaries.
- Solutions can be set to become **approximately periodic** in sufficiently large domains.
- Transform $\Phi = U_0(y)x + c_0(y) + \tilde{\Phi}$, where $\tilde{\Phi}$ is *x*-periodic, then solve the BLE for η and $\tilde{\Phi}$.



7. Simulation of extreme waves: initial conditions

BLE Initial condition consists of two (SP2) or three (SP3) line solitons, expressions of which are known from the KPE-solution:

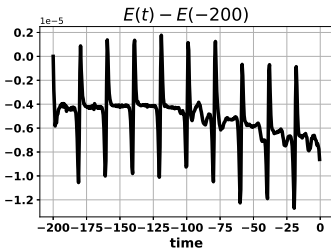
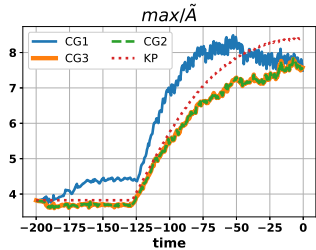
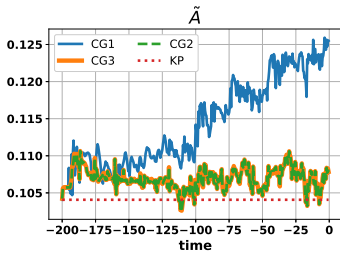
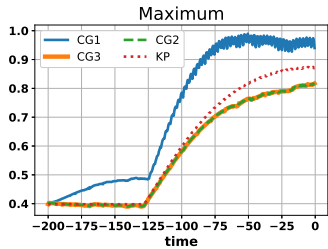
$$\eta_0(x, y) = \eta(x, y, t_0) = 2\left(\frac{4}{3}\right)^{1/3} \partial_{XX} \ln K(X, Y, \tau),$$

$$\varPhi_0(x, y) = \varPhi(x, y, t_0) = 2\sqrt{\epsilon} \left(\frac{4\sqrt{2}}{9}\right)^{1/3} \partial_X \ln K(X, Y, \tau).$$

Computational domain is constructed such that initial condition satisfies “periodic boundary conditions” in x -direction.

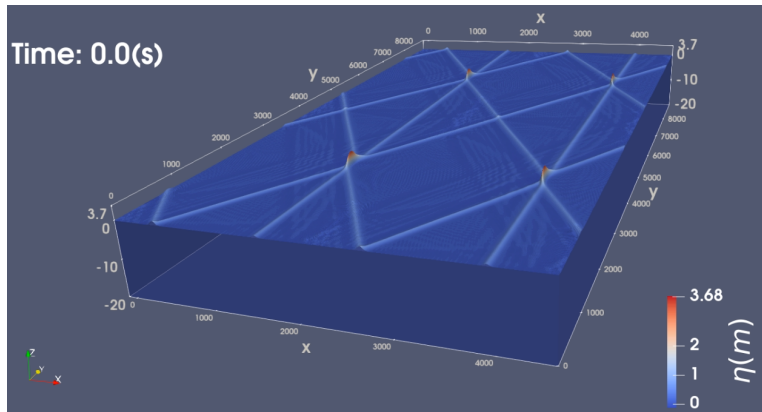
Case	L_x	L_y	T	N_x	N_y	$\Delta x = \frac{L_x}{N_x}$	$\Delta y = \frac{L_y}{N_y}$	Δt
SP2	10.3	40	50	132	480	0.0779	0.0833	0.005
SP3	20.9	47	200	252	564	0.0829	0.0833	0.005

7. Simulation of extreme waves: BLE SP3



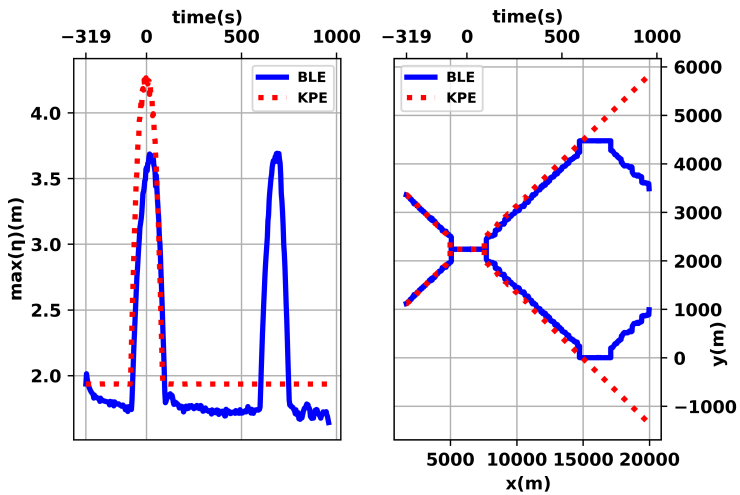
Results simulation three-soliton interaction (dimensional)

Crossing seas (4 or 8 domains combined – YouTube)



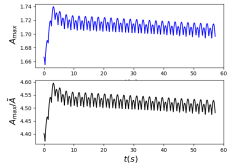
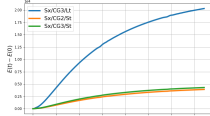
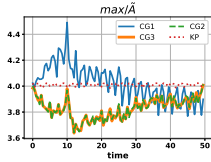
Results simulation three-soliton interaction (dimensional)

Cnoidal waves with periodicity in x, y, t (max. vs. t & $x-y$ tracks):



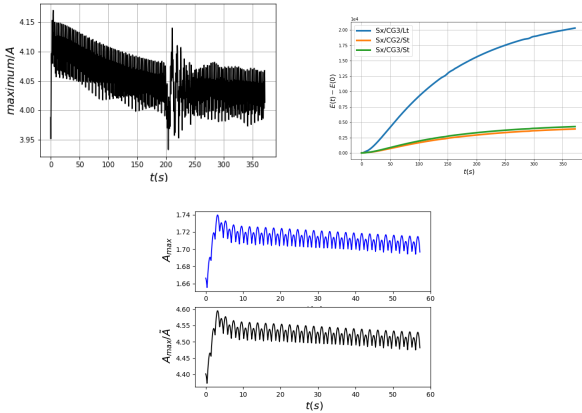
New results BLE- & PFE-simulations three-soliton interaction

- KPE with $\{\delta = 10^{-10}, 9^- \times\}$ seeding of BLE simulation yields **8.5× amplification** $t_{BLE} \in [-110, 0]$ (Junho Choi).
- PFE simulation based on 3+1D **discretisation of time-discrete variational principle (VP)** in Firedrake: robust, fast development, fewer human errors. MMP & SV time discretisations.
- Demanding **PFE simulations** in progress: HPC simulation with optimised ASM* pre-conditioner. *SP2*:



New results BLE- & PFE-simulations three-soliton interaction

- Demanding **PFE simulations** in progress: HPC simulation with optimised Additive Schwarz Method-Star pre-conditioner. *SP2*:



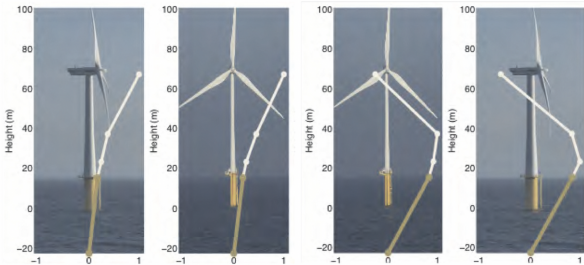
PFE-simulations SP1, SP2, SP3

VP with modified midpoint typed in phonetically (SP1 worked in 2 days, SP2/SP3 in few wks, ASM preconditioner by CC in one month –testing now):

$$\begin{aligned} 0 = & \delta \int_{\hat{\Omega}_{x,y}} \left[\left(-H_0 W \psi^{n+1/2} \frac{(h^{n+1} - h^n)}{\Delta t} + H_0 W \psi^{n+1} \frac{h^{n+1}}{\Delta t} - H_0 W \psi^n \frac{h^n}{\Delta t} \right. \right. \\ & + \frac{1}{2} H_0 g W (h^{n+1} (\frac{1}{2} h^{n+1} - H_0) + h^n (\frac{1}{2} h^n - H_0)) \Big) \\ & + \frac{1}{2} \int_0^{H_0} \left[\frac{1}{2} \frac{L_w^2}{W} h^{n+1} (\psi_x^{n+1/2} \hat{\phi} + \varphi_x^{n+1/2} - \frac{1}{h^{n+1}} (z h_x^{n+1}) (\psi^{n+1/2} \hat{\phi}_z + \varphi_z^{n+1/2}))^2 \right. \\ & + \frac{1}{2} W h^{n+1} \left(\psi_y^{n+1/2} \hat{\phi} + \varphi_y^{n+1/2} - \frac{1}{h^{n+1}} (z h_y^{n+1}) (\psi^{n+1/2} \hat{\phi}_z + \varphi_z^{n+1/2}) \right)^2 \\ & \left. \left. + \frac{1}{2} W \frac{H_0^2}{h^{n+1}} (\psi^{n+1/2} \hat{\phi}_z + \varphi_z^{n+1/2})^2 \right] dz \right. \\ & \left. + \frac{1}{2} W \frac{H_0^2}{h^n} (\psi^{n+1/2} \hat{\phi}_z + \varphi_z^{n+1/2})^2 \right] dz \right] dx dy. \end{aligned}$$

8. FSI asymptotic coordinate transformation for wind-turbine

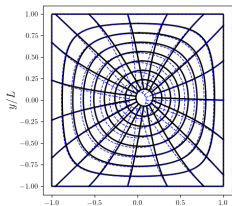
- Material deviation wind-turbine larger in horizontal but small in vertical (Ridder et al. 2017):



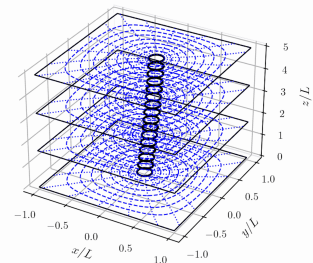
- Deviations from circular cross-section small, accumulation in horizontal larger.
- Elliptical-grid mapping* in horizontal at every z -level for FSI coupling.

8. FSI asymptotic coordinate transformation for wind-turbine

- *Elliptical-grid mapping* in horizontal at every z -level for FSI coupling:



(a)



(b)

FSI asymptotic coordinate transformation for wind-turbine

- Horizontal Lagrangian label coordinates a, b , centre or mass $X_0(z, t)$ at every z -level deviates:

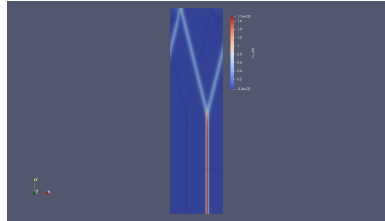
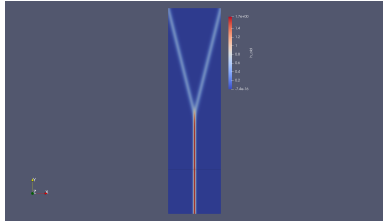
$$X_0(z, t) = \iint X(a, b, z, t) da db \quad \text{and} \quad Y_0(z, t) = \iint Y(a, b, z, t) da db$$

- Elliptical grid mapping: \sim circle centred at (X_0, Y_0) with radius $R(z)L$ wind turbine mast's cross-section to fixed domain $r \in [R, 1], \theta \in [0, 2\pi]$ with $R(z) \ll 1$:

$$\begin{aligned} u &= r \cos \theta, \quad v = r \sin \theta \\ \frac{x(r, \theta, z)}{L} &= \frac{1}{2} \sqrt{2 + u^2 - v^2 + 2\sqrt{2}u} - \frac{1}{2} \sqrt{2 + u^2 - v^2 - 2\sqrt{2}u} + \frac{(1-r)}{(1-R)} X_0(z, t) \\ \frac{y(r, \theta, z)}{L} &= \frac{1}{2} \sqrt{2 - u^2 + v^2 + 2\sqrt{2}v} - \frac{1}{2} \sqrt{2 - u^2 + v^2 - 2\sqrt{2}v} + \frac{(1-r)}{(1-R)} Y_0(z, t), \end{aligned} \tag{4}$$

9. Summary

- Nine-fold soliton amplification proven, with stable limit $\delta \rightarrow 0$.
- KPE amplification 8.4 & 9, **BLE simulation** at ~ 7.8 & 8.5.
- PFE (and BLE) simulations: convergence checks in progress.
- Extreme waves suitable for experimental validation (design).
- FSI between PFE & wind turbine, 2D then 3D;



References

- Choi, B, Kalogirou, Kelmanson (2022) *Water Waves* **4**.
<https://link.springer.com/article/10.1007/s42286-022-00059-3>
- B, Kalogirou, Zweers (2019) From bore-soliton-splash to a new wave-to-wire wave-energy model. *Water Waves* **1**.
- Gidel, B, Kalogirou (2017) Variational modelling of extreme waves through oblique interaction *Nonl. Proc. Geophys.* **24**.
- B, Kalogirou (2016) Variational Water Wave Modelling: from Continuum to Experiment. *Theory of Water Waves*, Bridges et al., *London Math. Soc.* **426**.
- Hairer, Lubich, Wanner (2006) *Geometric Numerical Integration*.
- Pego, Quintero (1999) 2D solitary waves of a BL equation. *Physica D* **132**.
- Crossing seas *YouTube movie*: <https://www.youtube.com/watch?v=EGhpQ7BM2jA>
- Korean Sejong Science project of Junho Choi & EU project w. Yang Lu & Wajiha Rehman
- Rehman et al 2023: two OMAE papers.

 Email: O.Bokhove@leeds.ac.uk (EU Eage: GA859983)